

# A Novel Approach to Fabricate Screen-Printed Electrode Based on The Composite of Gold Nanorods-Graphene Oxide for Detection of Uric Acid<sup>†</sup>

Wulan Tri Wahyuni<sup>1,2</sup>, Hana Safitri<sup>2</sup>, Eti Rohaeti<sup>2</sup>, Munawar Khalil<sup>3</sup> and Budi Riza Putra<sup>4\*</sup>

<sup>1</sup> Analytical Chemistry Division, Department of Chemistry, Faculty of Mathematics and Natural Sciences, IPB University, Indonesia

<sup>2</sup> Tropical Biopharmaca Research Center, Institute of Research and Community Empowerment, IPB University, Indonesia

<sup>3</sup> Department of Chemistry, Faculty of Mathematics and Natural Sciences, University of Indonesia, Indonesia

<sup>4</sup> Research Center for Metallurgy, National Research and Innovation Agency (BRIN), South Tangerang, Banten 15314

\* Correspondence: budiriza@gmail.com;

† Presented at The 2<sup>nd</sup> International Electronic Conference on Chemical Sensors and Analytical Chemistry, 16 – 30 September 2023. Online.

**Abstract:** In this work, we report the development of a technique to fabricate a screen-printed electrode (SPE) and its applications for uric acid sensing. The SPE was fabricated using a printing technique using an office printer printed on a photo paper substrate. Particularly, the conductive ink used for printing the working electrode (WE) and counter electrode (CE) consisted of graphene oxide (GO) and gold nanorod (AuNR) material. While the reference electrode (RE) was made by applying the conductive silver paste to the fabricated SPE. The electrochemical measurement of uric acid solution using fabricated SPE GO/AuNR provides a higher signal than the commercially available SPE. The electroanalytical performance of the fabricated SPE based on GO/AuNR toward the measurement of uric acid solution exhibited a linear range of 0.8–200  $\mu\text{M}$ , a detection limit of 0.5  $\mu\text{M}$ , a quantitation limit of 1.0  $\mu\text{M}$ , outstanding repeatability (% relative standard deviation) of 4.885 % as well as good selectivity with ascorbic acid, dopamine, glucose, urea, and sodium as interference. Furthermore, the fabricated SPE based on GO/AuNR was successfully employed for the determination of uric acid concentration in human urine samples using the standard addition approach.

**Keywords:** screen-printed electrode; gold nanorods; graphene oxide; uric acid; inkjet-printing

**Citation:** To be added by editorial staff during production.

Academic Editor: Firstname Last-name

Published: date

**Publisher's Note:** MDPI stays neutral with regard to jurisdictional claims in published maps and institutional affiliations.



**Copyright:** © 2022 by the authors. Submitted for possible open access publication under the terms and conditions of the Creative Commons Attribution (CC BY) license (<https://creativecommons.org/licenses/by/4.0/>).

## 1. Introduction

The determination of uric acid concentration in the sample of human body (urine and serum) is one of the important tests performed in the clinical laboratory due to as early diagnosis of diseases [1]. The standard method for detection of uric acid in clinical laboratories such as fluorescence and chemiluminescence has several drawbacks such as tedious, expensive reagents, the need for a trained person to operate the instruments, and difficulty in autonomous processes [2]. One alternative method that could be developed for rapid, reliable, and potentially be applied as early detection of uric acid analysis is the electrochemical method by utilizing a screen-printed electrode (SPE) instead of a traditional electrode [3]. SPE consists of a working electrode (WE), reference (RE), and counter electrode (RE) which can be fabricated by previously preparing ink conductive as electrode modifiers [4]. Among various fabrication techniques for SPE fabrication, the screen-printing technique using an office inkjet printer offers an interesting approach the large-

scale production due to the rapid, low-cost, scalable, easy-to-use, and versatile manufacturing process [5].

In this work, we have developed the fabrication of SPE based on composite materials consisting of graphene oxide and gold nanorods (AuNR) as electrode modifiers using a commercial inkjet printer. Graphene oxide has been extensively employed as electrode material due to its unique physicochemical properties such as high surface area, excellent thermal and electric conductivity, and possess wider potential for electrochemical investigations [6]. Meanwhile, gold nanorod (AuNR) has been reported could enhance electrode conductivity by making faster electron transfer and superior and increased analytical superior to be used for quantitative analysis, especially for uric acid sensors [7]. The developed uric acid sensor based on SPE-based GO/AuNR was then investigated by electrochemical methods such as cyclic voltammetry (CV) and differential pulse voltammetry (DPV) and finally tested in the sample of human urine. This novel materials combination for uric acid detection based on SPE using a commercial printer is expected could open a new avenue to be developed further as an early point-of-care device.

## 2. Materials and Methods

Graphite powder,  $\text{H}_2\text{SO}_4$ , gold(III) chloride hydrate ( $\text{HAuCl}_4 \cdot x\text{H}_2\text{O}$ ), hexadecyltrimethylammonium bromide (CTAB),  $\text{NaBH}_4$ ,  $\text{AgNO}_3$ , ethylene glycol, monobutyl ether (EGMBE), polyvinylpyrrolidone (PVP), L-(+)-ascorbic acid, and uric acid were obtained from Sigma Aldrich.  $\text{NaNO}_3$ ,  $\text{KMnO}_4$ ,  $\text{H}_2\text{O}_2$  30%, glycerol, KCl, and Triton X-100 were purchased from Merck (Darmstadt, Germany). Silver powder, paraffin block, and photo paper (merry professional glossy inkjet photo paper) were obtained from the local store. Commercial screen-printed carbon electrodes (SPCE) were purchased from DropSens (C110-NTC, Metrohm, DropSens). Deionized water was used in the throughout experiments.

The electrochemical experiments were performed using PalmSens Emstat3+ Blue. The graphene oxide (GO) sample was ground using Planetary Ball Mill PM 100. Raman spectrum of GO was obtained using HORIBA HR Evolution Raman Microscope with laser excitation wavelength at 514 nm. The absorbance spectrum of gold nanorod (AuNR) was obtained using a Genesys 10s UV-Vis Spectrophotometer. Transmission electron microscopy (TEM) images of GO and AuNR were obtained using TECNAI G2 Spirit Twin HR-TEM.

### 2.1. Synthesis of graphene oxide (GO) and gold nanorod (AuNR)

Graphene oxide was synthesized using Hummer's method based on the previously reported method [8]. The resulting GO powder was ground using a planetary ball mill for 5 hours at a speed of 70 rpm. Meanwhile, the synthesis of gold nanorod (AuNR) was following the seed-growth method based on the previously reported method [9]. Both GO powder and AuNR in deionized water were then mixed to prepare the conductive ink for the preparation of the screen-printed electrode (SPE).

### 2.2. Formulation of conductive ink for SPE fabrication

The pattern of SPE was designed using CorelDraw X7 with the reference following the template from commercial SPCE from Metrohm as displayed in Figure 1. The conductive ink for printing the working electrode (WE) and counter electrode (CE) consists of GO powder, AuNR, and organic solvents such as glycerol, ethylene glycol, and EGMBE. The composition of ink conductive for the preparation of SPE is as follows: GO (0.25% w/w), PVP (1.25% w/w), glycerol (30% w/w), ethylene glycol (20% w/w), EGMBE (2.5% w/w), Triton X-100 (0.25% w/w), and AuNR in water (50% w/w). Meanwhile, the ink conductive for reference electrode (RE) was prepared by mixing the silver powder with EGMBE for 2 minutes to obtain its final concentration of 20% w/w.

### 2.3. Fabrication of SPE based on the composite of GO/AuNR

The template of SPE was designed using CorelDraw X7 with the reference following the pattern of commercial SPCE provided by Metrohm as displayed in Figure 1A. The ink conductive was then inserted into the commercial office inkjet printer (Epson EcoTank L121 A4 Ink Tank Printer) with the substrate as photo paper. The printing of SPE was repeated 2 times to obtain the homogenous dispersion of ink conductive in the SPE pattern. Silver ink was applied to the pattern of SPE to fabricate the reference electrode. Then, the resulting SPE was dried in the oven for 3 minutes. Paraffin wax as an insulating layer was applied on top of the fabricated SPE and copper foil was inserted to give a connection path to WE, RE, and CE. Figure 1A displays the schematic illustration of the preparation of SPE based on GO/AuNR on the photo paper as a substrate. The resulting SPE based on GO/AuNR fabricated by inkjet printing is shown in Figure 1B.

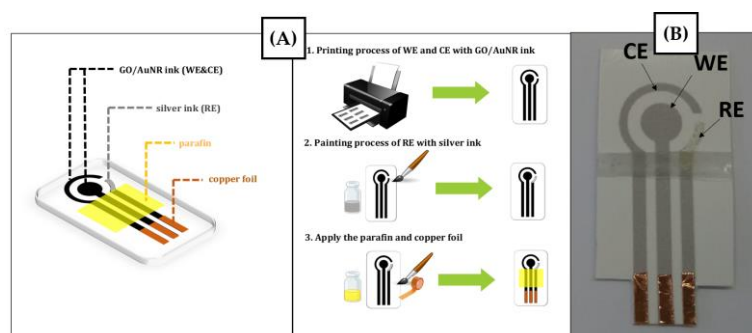


**Figure 1.** (A) Schematic illustration of the fabrication process of SPE based on GO/AuNR using inkjet-printing technique, (B) the result of the fabricated SPE with inkjet-printing technique.

### 2.4. Evaluation of the analytical performance of the fabricated SPE

The analytical performance of the fabricated SPE was evaluated in several parameters such as linearity, limit of detection (LOD), limit of quantitation (LOQ), reproducibility, stability, and selectivity. The evaluation of electroanalytical performance was performed using the solution of 0.2 mM uric acid in 0.1 M KCl electrolyte. To assess its applicability, the fabricated SPE was tested in a sample of human urine.

*Linearity, limit of detection, and limit of quantification.* Linearity was evaluated by preparing the uric acid solution in varied concentrations from 0.8 to 200  $\mu\text{M}$  in 0.1 M KCl as a supporting electrolyte. Each uric acid solution was scanned in triplicates using the differential pulse voltammetry (DPV) technique at a potential window from 0 to +0.8V, a scan rate of 50  $\text{mV s}^{-1}$ , a potential step of 5 mV, a potential pulse of 25 mV, and a pulse time of 0.01 s. The calibration curve from linearity was obtained with the relationship between the concentration of uric acid (x-axis) versus the anodic current of uric acid oxidation (y-axis). The value of LOD was derived from the ratio between signal versus noise (S/N) as 3:1. In addition, the LOQ value was determined by the ratio of S/N as 10:1.

*Reproducibility and stability.* The reproducibility was determined by measuring 50  $\mu\text{M}$  uric acid solution using five different electrodes of SPE based on GO/AuNR. Meanwhile, the sensor stability was evaluated by measuring 50  $\mu\text{M}$  uric acid solution for five consecutive days using a similar electrode. All electrochemical experiments were performed at optimum conditions using the DPV technique.

*Selectivity.* The selectivity was evaluated by measuring 50  $\mu\text{M}$  uric acid solution with the presence of several interfering species such as ascorbic acid, dopamine, urea, and sodium using the DPV technique. The experimental conditions used in the selectivity studies were at the potential range from 0 to +1V, a scan rate of 50  $\text{mV s}^{-1}$ , a potential step of 5 mV, a potential pulse of 25 mV, and a time pulse of 0.01 s.

*Analysis of Uric Acid in the Human Urine Samples.* The electroanalytical performance of SPE based on GO/AuNR for uric acid measurement was performed from a healthy human sample. The sample of human urine was diluted 50 times. Then, 5 mL of diluted

urine was spiked with the standard solution of uric acid in 0.1 M KCl to obtain the final concentration of 5 – 50  $\mu\text{M}$ . The sample of human urine was measured using the DPV technique at the potential range from 0 to +1V, a scan rate of 50  $\text{mV s}^{-1}$ , a potential step of 5 mV, a potential pulse of 25 mV, and a time pulse of 0.01 s. The concentration of uric acid in the sample of human urine was determined based on the linear regression equation of the standard addition method using the equation below:

$$x\text{-intersep} = -C_A \cdot (V_0/V_i)$$

where  $C_A$  is the spiked concentration of uric acid,  $V_0$  is the initial volume of the human urine sample before the spiking process, and  $V_i$  is the final volume of the human urine sample after the spiking process.

### 3. Results and Discussions

#### 3.1. Characterization of GO and AuNR

Raman analysis was performed to GO to identify the presence of 3 characteristic peaks of carbon-based materials which is D, G, and 2D bands. D band is associated with the presence of carbon  $sp^2$  which corresponds to the defect or vacancy in the carbon structure. Then, the G band is correlated with vibrations in  $sp^2$  hybridized-carbon atoms and the 2D band indicated the number of graphene layers [10]. As seen in Figure 1A, graphite shows several Raman peaks at 1575  $\text{cm}^{-1}$  (G band), 1347  $\text{cm}^{-1}$  (D band), and 2707  $\text{cm}^{-1}$  (2D band) which indicate the signature of carbon materials [11]. Meanwhile, when graphite was converted to GO, a higher intensity in the 2D band and a lower intensity in the G band are shown in its Raman spectra. This is due to the disturbance in graphite structure which resulted in the introduction of a new functional group such as carboxylic, hydroxyl, and epoxide [12]. In addition, the presence of oxygen atoms in graphite structure changes the hybridization from  $sp^2$  to  $sp^3$  [13]. Moreover, the ratio intensity of  $I_D/I_G$  was increased from 0.14 (graphite) to 1.08 (GO) which confirms the successful conversion of graphite to  $sp^3$ -hybridized carbon atoms in the graphene layer [14]. Furthermore, the reduced intensity of 2D from GO to graphite denotes the decreasing number of graphene layers in the GO structure.

FT-IR analysis was performed to observe the structural changes when graphite oxidized to GO materials by scanning in the infrared region (1000 – 4000  $\text{cm}^{-1}$ ). Based on IR spectra as shown in Figure 1B, the GO spectrum shows several vibration peaks at 3398  $\text{cm}^{-1}$  (O-H stretching), 1719  $\text{cm}^{-1}$  (C=O stretching), 1619  $\text{cm}^{-1}$  (C=C aromatic stretching), 1167  $\text{cm}^{-1}$  (C-O-C stretching), and 1036  $\text{cm}^{-1}$  (C-O stretching) [15,16]. The existence of these functional groups in GO indicates the structural changes in its graphene layers compared to a few absorption signals observed in graphite spectra [17].

TEM images were obtained from graphene oxide and the synthesized gold nanorods (AuNR) as shown in Figures 1C and D. It can be seen the morphology of graphene oxide resembles thin layers folded in the edges (Figure 1C) while the calculated ratio of length vs width of 300 AuNPs as 3.4 as displayed in Figure 1D.

#### 3.2. Fabrication of SPE based on GO/AuNR using an Inkjet-Printer

The composition of conductive ink was prepared by mixing 2.5 mg/mL of GO with 10 mL of AuNR solution with adding several additives such as glycerol, ethylene glycol, and ethylene glycol monobutyl ether (EGMBE). These organic solvents were added to obtain the homogenous and stable ink which can prevent GO precipitation resulting in an easier evaporation of composite solution on the SPE template [18]. Polyvinyl pyrrolidone (PVP) was also added to the mixture of conductive ink as a binder while Triton X-100 has a function to reduce the surface tension of the composite [19]. The resulting viscosity of conductive ink is 5 mPa s which resembles the viscosity of a commercial ink printer. Prior to the insertion of the prepared conductive ink into the inkjet printer, the composite solution was filtered with a syringe filter PVDF 0.45  $\mu\text{m}$  to remove any small particulates. Then, this conductive ink based on GO/AuNR was employed to fabricate the working

electrode (WE) and the counter electrode (CE). Meanwhile, silver ink was applied to the SPE pattern to fabricate the reference electrode (RE) and dried in the oven at 80 °C to make sure the ink solvent completely evaporated. The last step of SPE fabrication is to apply paraffin wax to define the surface area of electrode and the conductive pathway produced by connecting copper foil to the WE, RE, and CE.

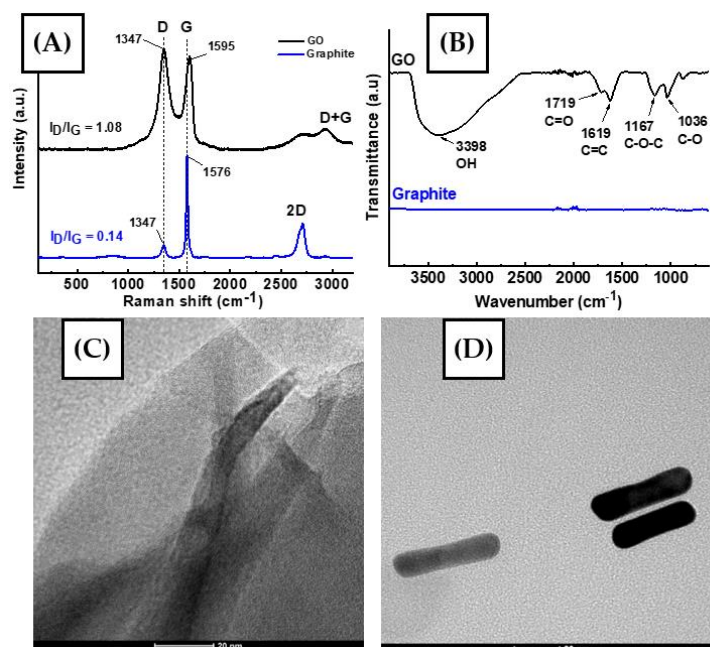


**Figure 2.** The spectrum of graphite and graphene oxide (GO) for (A) Raman and (B) FT-IR, TEM images for (C) GO, and (D) gold nanorod (AuNR).

### 3.3. Electrochemical investigation of uric acid oxidation using SPE-based GO/AuNR

The electrochemical performance of commercial SPCE and SPE-based GO/AuNR was evaluated by measuring 0.2 mM uric acid in 0.1 M KCl using both voltammetric techniques (CV and DPV). The parameters used for the CV technique were similar at a potential range from 0 to +0.5 V (vs. Ag/AgCl), a potential step of 0.005 V, and a scan rate of 50 mV s<sup>-1</sup>. It can be seen from Figure 3A, the anodic peak of uric acid oxidation was observed at 0.38 V (vs. Ag/AgCl) using commercial SPCE and at 0.25 V (vs. Ag/AgCl) using SPE-based GO/AuNR. In addition, the observed current of uric acid oxidation at SPE-based GO/AuNR is shown 7 times higher than measured with commercial SPCE.

Next, DPV was chosen to further investigate uric acid oxidation due to its higher sensitivity by reducing capacitive current to provide sharper oxidation current compared with other voltammetric techniques [20]. Prior to the measurements using SPE-based GO/AuNR, it was pretreated by applying the CV technique in 20 cycles using 0.2 mM uric acid in 0.1 M KCl to enhance its sensitivity. The parameters used in DPV for uric acid measurements were at a potential from 0 to 0.8 V (vs. Ag/AgCl), at a potential step of 0.005 V, a potential pulse of 0.025 V, and at a scan rate of 50 mV s<sup>-1</sup>. Based on Figure 3B, it can be seen the oxidation peak of uric acid shifted to a more negative potential (0.25 V vs. Ag/AgCl) with a sharper and higher intensity of current. This is due to the electrocatalytic effect from the composite of GO/AuNR which results in increasing sensitivity for uric acid measurements using the proposed sensor [21]. It can be deduced the enhanced electrocatalytic activity of GO/AuNR composite derived from that the role of GO by forming hydrogen bonding and  $\pi$ - $\pi$  interactions toward uric acid while AuNR is an electron transfer channel to the surface of modified electrode [22].

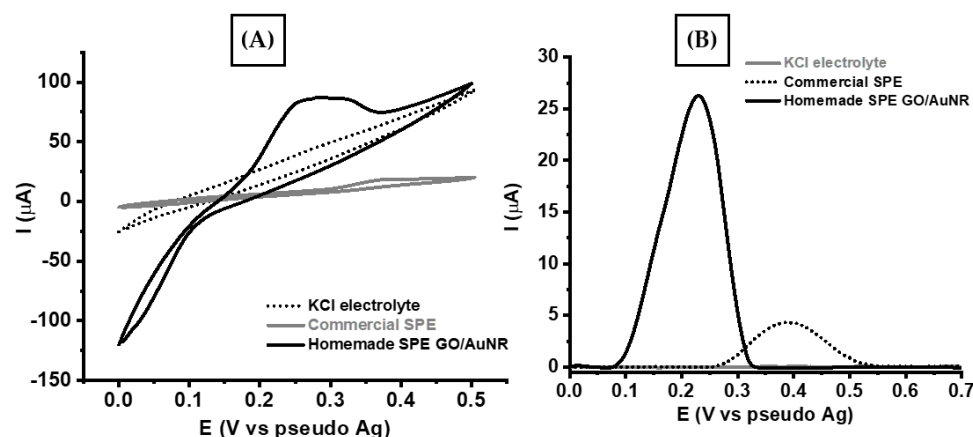


**Figure 3.** Voltammograms were obtained from (A) CV and (B) DPV techniques for the measurements of 0.2 mM uric acid in 0.1 M KCl using commercial SPCE and SPE based-GO/AuNR.

### 3.4. Analytical performance of SPE-based GO/AuNR

The electrochemical performance of SPE-based GO/AuNR has been evaluated in several analytical performances such as linearity, limit of detection (LOD), limit of quantification (LOQ), reproducibility, stability, and selectivity. Based on Figure 4A, it is clear the peak current linearly increased with the increasing concentration of uric acid. There are 2 linear regression equations obtained from DPV measurements of uric acid in a concentration range of 0.2 – 10  $\mu\text{M}$  ( $I_{pa}$  ( $\mu\text{A}$ ) = 0,3086 ( $\mu\text{M}$ ) + 0,9522;  $R^2 = 0,9979$ ) and 10 – 200  $\mu\text{M}$  ( $I_{oks}$  ( $\mu\text{A}$ ) = 0,1336 ( $\mu\text{M}$ ) + 1,4472 ( $R^2 = 0,9911$ )). All measurements of uric acid were performed in triplicate experiments. Then, it can be calculated the values of LOD and LOQ are 0.5  $\mu\text{M}$  and 1.0  $\mu\text{M}$ , respectively. In addition, Table 1 shows the comparison of electroanalytical performance of the proposed sensor for the uric acid sensor with previously reported sensors. It can be seen from this table, the proposed sensor displays a comparable performance in terms of linear range, LOD, and LOQ from the other sensors.

The reproducibility of the proposed sensor has been evaluated by measuring 50  $\mu\text{M}$  uric acid in 0.1 M KCl using 5 different electrodes. Based on Figure 4B, it was obtained a value of relative standard deviation (RSD) of 4.89%. Meanwhile, the electrode stability was investigated by measuring 50  $\mu\text{M}$  uric acid in 0.1 M KCl for 5 consecutive days and resulting in an RSD value of 7.42% as shown in Figure 4C. Furthermore, the sensor selectivity was studied by measuring 50  $\mu\text{M}$  uric acid in 0.1 M KCl in the presence of several interfering species such as ascorbic acid, dopamine, glucose, urea, and sodium. As shown in Figure 4D, the response current of SPE-based GO/AuNR displays a negligible change when the interfering species was added to an equal concentration of uric acid. This indicates that the proposed sensor could maintain its current response in the presence of interfering species. In addition, Table 2 displays the value of relative standard deviation (RSD) in the range of 94 – 110% which is acceptable in the analytical range. Therefore, it can be concluded that the proposed uric acid sensor shows good reliability for sensing purposes and may have the potency to be applied in real samples.

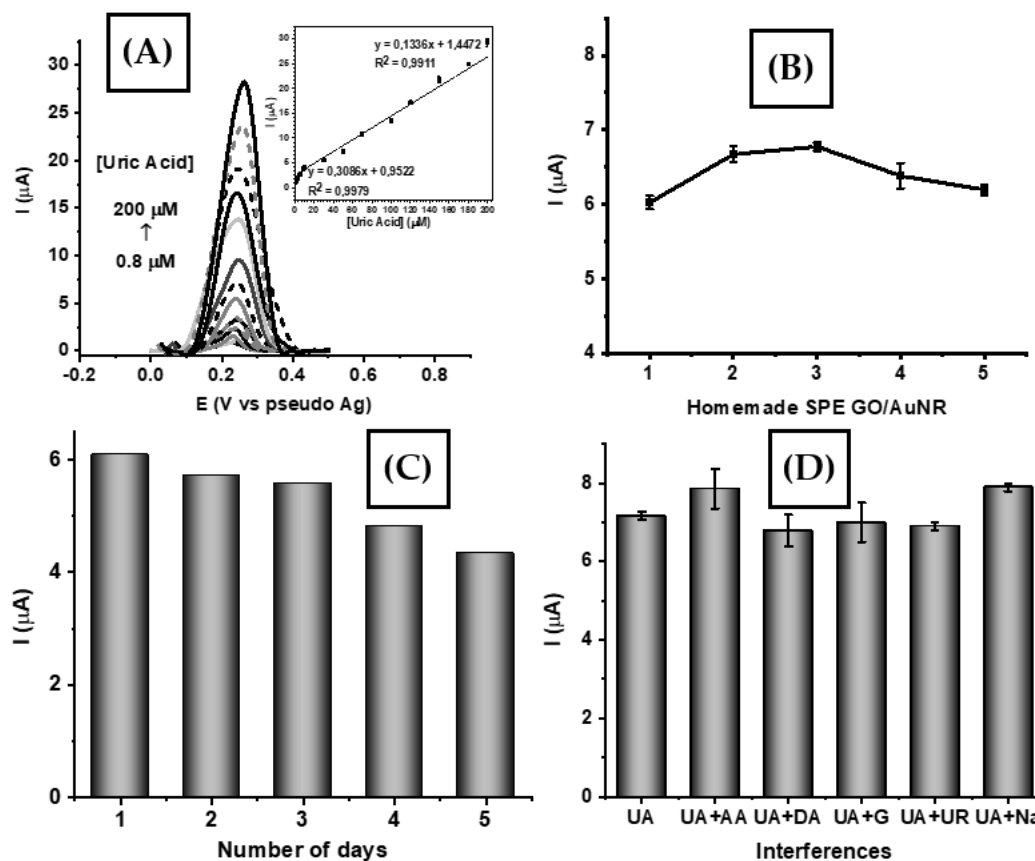


**Figure 4.** (A) Voltammograms obtained from the uric acid measurements in different concentrations (0.8 – 200  $\mu\text{M}$ ) in 0.1 M KCl using SPE-based GO/AuNR. Inset: the linear regression between peak current with uric acid concentration, (B) Reproducibility of uric acid measurements of 50  $\mu\text{M}$  using five different electrodes, (C) Stability of uric acid measurements at a concentration of 50  $\mu\text{M}$  over 5 days consecutive days, (D) Variation of response current in the uric acid measurement in the presence of several interferences such as ascorbic acid (AA), dopamine (DA), glucose (G), urea (UR), and sodium (Na) when measured with SPE-based GO/AuNR.

**Table 1.** Comparison of analytical performance of the proposed sensor or uric acid with other sensors.

Electrode	Linear range ( $\mu\text{M}$ )	LOD ( $\mu\text{M}$ )	LOQ ( $\mu\text{M}$ )	Ref.
Co-N/Zn@NPC <sup>1</sup>	0.1 – 14.7	$5 \times 10^{-4}$	$1.6 \times 10^{-3}$	[23]
PCL/PEI/UOx/QD <sup>2</sup>	5 – 52.0	3.96	13.1	[24]
Poly(DPA) <sup>3</sup> SiO <sub>2</sub> @Fe <sub>3</sub> O <sub>4</sub>	1.2 – 1.8	0.4	1.2	[25]
Chi/GOx/PB-G <sup>4</sup>	10 – 30	0.11	0.38	[26]
OXL-9 <sup>5</sup>	40 – 120	1.4	4.7	[27]
ErGO/PEDOT:PSS <sup>6</sup>	10 – 100	1.08	3.61	[28]
rGO/AuNPs	10 – 500	3.6	10.95	[29]
MC-GO <sup>7</sup> -Fe <sub>3</sub> O <sub>4</sub>	0.5 – 140	0.17	0.5	[30]
GO/AuNR	0.8 – 200	0.5	1.0	This work

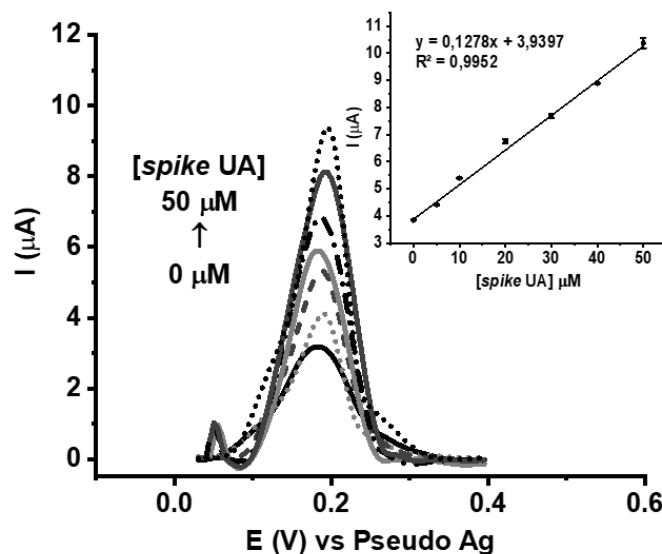
<sup>1</sup> Nanoporous carbon. <sup>2</sup> Polycaprolactone/polyethylene imine/uricase/quantum dot. <sup>3</sup> dipicolinic acid. <sup>4</sup> chitosan/glucose oxidase/Prussian blue-graphite. <sup>5</sup> Octoxynol-9. <sup>6</sup> Electrochemically reduced graphene oxide/poly(3,4-ethylenedioxythiophene):poly(styrenesulfonate). <sup>7</sup> Methylcellulose/graphene oxide.

**Table 2.** The effect of interference in the selectivity studies and its recovery values for the measurement of 50  $\mu\text{M}$  uric acid.

Interference	The concentration ratio (uric acid: interference)	Iox uric acid ( $\mu\text{A}$ )	% Recovery
-	-	$7.162 \pm 0.2$	-
Ascorbic acid	1 : 1	$7.855 \pm 0.8$	$109.7 \pm 1.9$
Dopamine	1 : 1	$6.789 \pm 0.7$	$94.8 \pm 12.6$
Glucose	1 : 1	$6.997 \pm 0.8$	$97.7 \pm 13.6$
Urea	1 : 1	$6.902 \pm 0.1$	$96.4 \pm 3.6$
Sodium	1 : 1	$7.893 \pm 0.2$	$110.2 \pm 5.3$

### 3.5. Analysis of real samples

The proposed uric acid sensor (SPE-based GO/AuNR) was employed for uric acid determination in the sample of human urine. Initially, the human urine sample was diluted 50 times and spiked with uric acid using the standard addition method. Figure 5 displays the resulting voltammogram of uric acid measurements from the human urine sample using the standard addition method with the corresponding calibration plot ( $y = 0.1278x + 3.9397$ ;  $R^2 = 0.9952$ ). Based on this regression equation, it can be calculated the concentration of uric acid in the sample of human urine as 3.086 mM. The uric acid concentration in the sample of human urine was also determined in the clinical laboratory and reported as 3.45 mM. Therefore, it can be concluded that SPE-based GO/AuNR may have a potency to be employed in the real application as uric acid sensor.

**Figure 5.** Voltammogram response of the sample of human urine spiked with increasing concentration of uric acid (0 – 50  $\mu\text{M}$ ) in 0.1 M KCl measured using SPE-based GO/AuNR. The inset is the resulting calibration plot.

## 4. Conclusions

This work summarizes the fabrication of screen-printed electrode (SPE)-based on GO/AuNR composite has been demonstrated using a commercial inkjet printer for uric acid detection. The fabricated uric acid sensor shows good analytical performance in terms of linearity (0.8 – 200  $\mu\text{M}$ ), limit of detection (0.5  $\mu\text{M}$ ), and limit of quantification (1.0  $\mu\text{M}$ ) when it was investigated using the differential pulse voltammetry (DPV) technique. In addition, the fabricated uric acid sensor also shows acceptable reproducibility, stability, and selectivity in the presence of several potential interfering ions such as ascorbic acid, dopamine, glucose, urea, and sodium). The proposed sensor was ultimately applied to

detect uric acid concentration in the sample of human urine which is its performance also comparable with the result obtained from the clinical laboratory. Thus, it can be inferred that the developed method for uric acid detection using SPE-based GO/AuNR may have a potency to be applied in real applications.

**Author Contributions:** B. R. P.: methodology, writing-review, and editing, supervision, H. S: draft preparation, data curation, methodology, W. T. W: funding acquisition, supervision, E. R.: supervision, M. K.: review, editing. All authors have read and agreed to the published version of the manuscript.

**Funding:** This research received no external funding.

**Institutional Review Board Statement:** Not applicable

**Informed Consent Statement:** Not applicable

**Data Availability Statement:** Not applicable.

**Conflicts of Interest:** The authors declare no conflict of interest.

## References

1. Moravcik, O., Dvorak, M., Kuban, P., Autonomous capillary electrophoresis processing and analysis of dried blood spots for high-throughput determination of uric acid. *Anal. Chim. Acta.* 2023, 1267, 341390.
2. Wang, Q., Wen, X., Kong, J., Recent progress on uric acid detection: a review. *Crit. Rev. Anal. Chem.* 2020, 50(4), 359-375.
3. Verman, G., Singhai, S., Rai, P. K., Gupta, A., A simple approach to develop a paper-based biosensor for real-time uric acid detection. *Anal. Methods.* 2023, 15, 2955-2963.
4. Wahyuni, W T., Putra, B. R., Heryanto, R., Rohaeti, E., Yanto, D. H. Y., Fauzi, A., A simple approach to fabricate a screen-printed electrode and its application for uric acid detection. *Int. J. Electrochem. Sci.*, 2021, 16, 210221.
5. Liu, Y., Hao, J., Zheng, X., Shi, C., Yang, H., Screen printing of stretchable silver nanomaterial inks for a stable human-machine interface. *J. Mater. Chem. C.* 2023, 11, 5009-2017.
6. Anindya, W., Wahyuni, W. T., Rafi, M., Putra, B. R., Electrochemical sensor based on graphene oxide/PEDOT:PSS composite modified glassy carbon electrode for environmental nitrite detection. *Int. J. Electrochem. Sci.* 2023, 18(3), 100034.
7. Husna, R., Kurup, C. P., Ansari, M. A., Mohd-Naim, N. F., Ahmed, M. U., An electrochemical aptasensor based on AuNRs/AuNWs for sensitive detection of apolipoprotein A-1 (ApoA1) from human serum. *RSC Adv.* 2023, 13, 3890-3898.
8. Akhavan, O.; Bijanzad, K.; Mirsepah, A. Synthesis of graphene from natural and industrial carbonaceous waste. *RSC Adv.* 2014, 4, 20441-20448.
9. Nikoobakht, B., El-Sayed, M. A. Preparation and growth mechanism of gold nanorods (NRs) using seed-mediated growth method. *Chem. Mater.* 2002, 15, 10, 1957-1962.
10. Oliveira, A. E. F., Braga, G. B., Tarley, C. R. T., Pereira, A. C. Thermally reduced graphene oxide: synthesis, studies and characterization. *J. Mater. Sci.* 2018, 53, 12005-12015.
11. Ossoon, B. D., Belanger, D. Synthesis and characterization of sulfophenyl-functionalized reduced graphene oxide sheets. *RSC Adv.* 2017, 7, 27224-27234.
12. Khine, Y. Y., Wen, X., Jin, X., Foller, T., Joshi, R., Functional groups in graphene oxide. *Phys. Chem. Chem. Phys.* 2022, 24, 26337-26355.
13. Muzyka, R., Drewniak, S., Pustelny, T., Chrubasik, Gryglewicz, G., Characterization of graphite oxide and reduced graphene oxide obtained from different graphite precursors and oxidized by different methods using Raman spectroscopy. *Materials.* 2018, 11(7), 1050.
14. Vecera, P., Eigler, S., Kolesnik-Gray, M., Krstic, Vierck, A., Maultzsch, J., Schafer, R. A., Hauke, F., Hirsch, A., Degree of functionalization dependence of individual Raman intensities in covalent graphene derivatives. *Sci. Rep.* 2017, 7, 45165.
15. Larraza, I., Ugarte, L., Fayanas, A., Gabilondo, N., Arbelaiz, A., Corcuera, M. A., Eceiza, A., Influence of process parameters in graphene oxide obtention on the properties of mechanically strong alginate nanocomposites. *Materials.* 2020, 13(5), 1081.
16. Shahriary, L., Athawale, A. A., Graphene oxide synthesized by using modified Hummers approach. *Int. J. Renew. Energy Environ.* 2014, 2, 1, 58-63.
17. Li, J., Yan, Q., Zhang, X., Zhang, J., Cai, Z., Efficient conversion of lignin waste to high value bio-graphene oxide nanomaterials. *Polymers.* 2019, 11(4), 623.
18. Li, Y.-L., Guo, X., Feng, X.-J., Li, L.-H., Graphene oxide for inkjet-printing technology. *Appl. Mech. Mater.* 2015, 748, 77-80.
19. Li, P., Cheng-An, T., Wang, B., Huang, J., Li, T., Wang, J., Preparation of graphene oxide-based ink for inkjet printing. *J. Nanosci. Nnaotechnol.* 2018, 18(1), 713-718.
20. Molazemhosseini, A., Magagnin, L., Vena, P., Liu, C.-C., Single-use disposable electrochemical label-free immunosensor for detection of glycosylated hemoglobin (HbA1c) using differential pulse voltammetry (DPV). *Sensors.* 2016, 16(7), 1024.
21. Safitri, H., Wahyuni, W. T., Rohaeti, E., Khalil, M., Marken, F., Optimization of uric acid detection with Au nanorod-decorated graphene oxide (GO/AuNR) using response surface methodology. *RSC Adv.* 2022, 12, 25269-25278.

22. Azimzadeh, M., Rahaie, M., Nasirizadeh, N., Ashtari, K., Naderi-Manesh, H., An electrochemical nanobiosensor for plasma miRNA-155, based on graphene oxide and gold nanorod, for early detection of breast cancer. *Biosens. Bioelectron.* 2016, 77, 99-106.
23. Shanmugam, R., Aniruthan, S., Yamunadevi, V., Nellaiappan, S., Amali, A. J., Suresh, D., Co-N/Zn@NPC derived from bimetallic zeolitic imidazolate frameworks: A dual mode simultaneous electrochemical sensor for uric acid and ascorbic acid. *Surf. Interfaces.* 2023, 40, 103103.
24. Muhammad, F., Dik, G., Kolak, S., Gedik, K. K., Bakar, B., Ulu, A., Ates, B., Design of highly selective, and sensitive screen-printed electrochemical sensor for detection of uric acid with uricase immobilized polycaprolactone/polyethylene imine electrospun nanofiber. *Electrochim. Acta.* 2023, 439, 141675.
25. Reddy, Y. V. M., Sravani, B., Agarwal, S., Gupta, V. K., Madhavi, G., Electrochemical sensor for detection of uric acid in the presence of ascorbic acid and dopamine using the poly(DPA)/SiO<sub>2</sub>@Fe<sub>3</sub>O<sub>4</sub> modified carbon paste electrode. *J. Electroanal. Chem.* 2018, 820, 168-175.
26. Soleh, A., Kanatharana, P., Thavarungkul, P., Limbut, W., Novel electrochemical sensor using a dual-working electrode system for simultaneous determination of glucose, uric acid, and dopamine. *Microchem. J.* 2020, 153, 105479.
27. Charithra, M. M., Manjunatha, J. G. G., Raril, C., Surfactant modified graphite paste electrode as an electrochemical sensor for the enhanced voltammetric detection of estriol with dopamine and uric acid. *Adv. Pharm. Bull.* 2020, 10(2), 247-253.
28. Putra, B. R., Nisa, U., Heryanto, R., Rohaeti, E., Khalil, M., Izzataddini, A., Wahyuni, W. T., A facile electrochemical sensor based on a composite of electrochemically reduced graphene oxide and a PEDOT:PSS modified glassy carbon electrode for uric acid detection. *Anal. Sci.* 2022, 38, 157-166.
29. Mazzara, F., Patella, B., Aiello, G., O'Riordan, A., Torino, C., Vilasi, A., Inguanta, R., Electrochemical detection of uric acid and ascorbic acid using r-GO/NPs based sensors. *Electrochim. Acta.* 2021, 388, 138652.
30. Sohoul, E., Khosrowshahi, E. M., Radi, P., Naghian, E., Rahimi-Nasrabadi, M., Ahmadi, F., Electrochemical sensor based on modified methylcellulose by graphene oxide and Fe<sub>3</sub>O<sub>4</sub> nanoparticles: Application in the analysis of uric acid content in urine. *J. Electroanal. Chem.* 2020, 877, 114503.